Desalination and Water Treatment
www.deswater.com

doi:10.5004/dwt.2017.21054

82 (2017) 369–378
July

Feasibility study on decontamination of aged spent wash using activated carbon from *Limonia acidissima* shell

K. Padmanabhan[a], M. Vasudevan[a,*], S. Ramakrishnan[a], N. Natarajan[b]

[a]*Department of Civil Engineering, Bannari Amman Institute of Technology, Sathyamangalam, Erode, Tamil Nadu, India-638401, email: vishnukswamy@gmail.com (K. Padmanabhan), Tel. +914295 226112, Fax +914295 226666, email: devamv@gmail.com, vasudevan@bitsathy.ac.in (M. Vasudevan), ramakrishnans@bitsathy.ac.in (S. Ramakrishnan)*
[b]*Department of Civil Engineering, Dr. Mahalingam College of Engineering and Technology, Pollachi, Tamil Nadu, India-642003, email: itsrajan2002@yahoo.co.in*

Received 1 February 2017; Accepted 14 June 2017

ABSTRACT

Need for eco-friendly and economical treatment of distillery spent wash has been inspiring researchers to investigate decontamination potential using natural materials. In this study, activated carbon was prepared from wood apple (*Limonia acidicima*) shells by thermo-chemical treatment with sulfuric acid at 200°C for 2 h in the absence of air. From the batch experiments with aged spent wash samples, maximum adsorption capacity (46.6 mg/g) was observed at a pH of 5.5, owing to the initial high uptake rate of polar compounds from spent wash. Based on the results from batch kinetic studies, two-site series and parallel interface models were found to be appropriate for representing the multi-phase transitions in the mass transfer rate. Comparison between different linear forms of Langmuir and Redlich-Peterson (R-P) isotherms revealed that prediction of adsorption capacity term is considerably affected by the axial setting in the logarithmic form. In order to overcome the difficulty of linear regression fit, chi-square test was identified as the suitable alternative to make comparison of all isotherms on the same abscissa and ordinate. Results of the present study showed that R-P isotherm and two-site interface kinetic models were invariably best suited for explaining the equilibrium and kinetic sorption of spent wash.

Keywords: Activated carbon; Adsorption; Non-linear isotherm; Spent wash; Two-site kinetic model; Wood apple

1. Introduction

Despite advent of stringent regulations and safety guidelines, discharge of industrial wastewater into natural water bodies is being practiced as a preferred method of disposal, virtually since the beginning of human civilization [1,2]. There are many literatures confirming deleterious environmental impact of waste-loading upon the receiving system either in terms of threat to aquatics, spreading of many contagious diseases and aquifer contamination [3,4]. Alcohol distilleries have been listed at the top in the 'Red category' of industries by Ministry of Environment and Forest (MoEF), Government of India owing to their highly polluting impact on the environment [5]. Nonetheless, distillery industry has surfaced as an important sector worldwide due to the large-scale applications of ethanol and distilled spirits in pharmaceuticals and food products [6].There are more than 319 distilleries currently operating in India, producing about 3.25×10^9 L of alcohol while generating 40.4×10^{10} L of wastewater annually [7,8].

As an unavoidable outcome of the alcohol brewing process, a brownish green, viscous, low-pH liquid called spent wash is generated as waste [9]. Spent wash typically contains high concentrations of organic matter in terms of chemical oxygen demand (COD) (60,000–1,00,000 mg/L), biochemical oxygen demand (BOD) (35,000–60,000 mg/L), inorganic matter as total solids (35,000–47,000 mg/L) and sulphate (980–5100 mg/L) with an extremely acidic pH (3.0–4.5) [5,6]. Spent wash also contains the major plant

*Corresponding author.

nutrients like total phosphorous (400–600 mg/L), total potassium (10,000–13,000 mg/L), total calcium (2,100–3,000 mg/L), total magnesium (2,000–3,300 mg/L), total sulphur (4,000–5,000 mg/L) and heavy metals such as iron, manganese, zinc [10]. It is well understood that presence of dark brown pigment (melanoidin) generated through the reaction between sugar and amino compounds (known as Maillard reaction) imparts colour to the water [10]. However, due to its recalcitrant nature, conventional wastewater treatment methods fail to achieve simultaneous decolourization and decontamination [7,8,10]. Use of indigenous and commercially prepared adsorbents has been reported as promising alternatives, and therefore, more focus is ascribed towards improvising their performance efficiency [11,12].

Eco-friendly as well as economical treatment of distillery spent wash in the developing countries has been attempted by many researchers. Bio-methanation followed by aerobic treatment is the general practice for treatment of distillery wastewater [13]. It was reported that aerobic treatment reduced COD and BOD up to 50–70% [14]. Microbial treatment using specially acclimatized microbial consortium has also been reported frequently in the recent years [15,16]. In recent years, several basidiomycetes and ascomycetes type fungi have been used in decolourisation of natural and synthetic melanoidins from distilleries [17].

Pre-treatment of spent wash with ceramic membranes prior to anaerobic digestion is reported to reduce the COD loading from 36,000 to 18,000 mg/L [18]. Wet air oxidation has been recommended as part of a combined process scheme for treating anaerobically digested spent wash [19]. Kumaresan et al. employed emulsion liquid membrane technique in a batch process for spent wash treatment [20]. Nataraj et al. reported pilot trials on distillery spent wash using a hybrid nano-filtration (NF) and RO process [21]. Chemical oxidation of effluent with chlorine resulted in 49% colour removal but the result was only temporary [22]. Beltran et al. reported that advanced oxidation of the effluent in combination with UV radiation enhanced spent wash degradation in terms of COD reduction; however ozone with hydrogen peroxide showed marginal reduction even for diluted effluent [23]. Photocatalytic oxidation has also been employed using solar radiation and TiO_2 as the photocatalyst [24].

Among the various tertiary treatment technologies, pollution abatement through adsorption studies has gained interest over the last few decades [25]. Adsorption onto activated carbon (AC) is the most effective and widely used technique in treating high strength wastewater due to its large surface area, high adsorption capacity and high degree of surface reactivity, resulting in fast mass transfer kinetics thereby simplifying the reactor design as compared to the other materials [26].

The preparation of activated carbon from natural materials has led to many scientific advances particularly in the development of surface activation and characterization methods. Several coals [27]; polymers [28], agricultural by-products and forest wastes [29,30] have been successfully employed as raw materials to prepare activated carbon. Uses of H_3PO_4, KOH and $ZnCl_2$ as activating agents for various nutshell species were also being studied. Hu and Vansant [31] reported wide range of pore size distribution of activated carbon from walnut shell char using KOH in the absence of air at 500–900°C. Preparation of activated carbon from cork waste using KOH at 800°C for 2 h yielded surface area of 1415 m^2/g [32]. Guo and Lua [33] produced activated carbon from peanut hull and oil palm stones using H_3PO_4, KOH and $ZnCl_2$ and activated at 500°C and 650°C respectively. Heidariet al. [34] prepared highly micro-porous activated carbon from *Eucalyptus camaldulensis* wood by chemical activation with H_3PO_4 and $ZnCl_2$ at different impregnation ratios as well as by pyrolysis, followed by activation with KOH.

Many researchers have attempted to assess pollutant removal efficiency of distillery spent wash using various agro-industrial materials such as activated charcoal [35], wood charcoal [36], fly ash and wood ash [37,38]. It is widely accepted that activated carbon can be used as a potential adsorbent for treating distillery wastewater. Although many agricultural waste materials have been identified for synthesizing activated carbon, usage of dried shells of wood apple (*Limonia acidicima* shell-LAS) has not been studied yet for treating distillery wastewater. The wood apple fruit is largely consumed by people of South-East Asia due to its dietary and medicinal importance; however, it is observed that the hard outer shell is generally discarded. In the absence of proper waste management system, open disposal of large amounts of shells directly in the soil may leave the residue in the environment for long duration due to their recalcitrant nature. This may lead to elution of various toxic compounds generated from polar functional groups such as alcoholic, carboxylic, and ethercompounds [39].

The choice of activation for preparing adsorbent largely depends on the physical-chemical nature as well as the strength of target contaminants. Many times, simple pre-treatment steps will make the substance ready for use as biosorbent, while a combination of physical-chemical and thermal treatments are required for optimizing the surface characteristics of activated carbon. Biopolymers extracted from sewage sludge have been successfully used as biosorbents for the removal of heavy metals such as Pb^{2+} and Zn^{2+} [4,40]. The removal rate of Pb^{2+} increased with the corresponding increase in the system pH [41]. The biopolymers with different proportions of proteins, polysaccharides and nucleic acids showed different adsorption capacities for Cu^{2+} [42]. Wood apple shell has been used both as biosorbent and as activated carbon for the removal of heavy metals [39,43–45]. Even though it is studied for the removal of methylene blue dye [46], there is no literature evidence of using LAS for decontamination and decolorization of distillery spent wash. In order to test this hypothesis, the present work is being carried out with objective to explore the viability of using thermo-chemically activated carbon derived from wood apple (LAS-AC) as a possible candidate for the reduction of COD from aged distillery spent wash.

2. Materials and methods

2.1. Preparation of LAS-AC

Among various methods to prepare activated carbon, activation with H_2SO_4 resulted in less moisture, moderate

conductivity and large surface area (229.67 m^2/g) of adsorbent having high adsorption capacity at pH of 5.7 [47]. The wood apple fruit shells were collected from local yards in and around Coimbatore, Tamil Nadu. The collected shells were washed, dried and rendered free from pulp and the outer rind was grinded to small pieces (1–3 cm size). These were soaked in 98% H_2SO_4 for 24 h and further, thermally activated at 200°C for 2h in a muffle furnace. After cooling to room temperature, the activated carbon was washed thoroughly with distilled water till the pH of the wash water turned out to be between 5 and 7. A good reason for maintaining a low pH is to minimize the impact of shock loading on the surface sites when subjected to strong acidic spent wash solutions [47]. This process of neutralizing the pH was accelerated by spiking few droplets of 0.1 N NaOH followed by rinsing the materials. Finally it was dried at 105°C for 4 h to make it ready for batch experiments.

2.2. Stock spent wash

The raw spent wash was collected from the distillery that was stored in a closed reinforced concrete tank for about a month. The physic-chemical characteristics were determined after it was diluted to about 1 ml in 1000 ml of water. It was highly turbid, heavily colored and odorous with a pH of about 4.5 and COD value of 120,000 mg/L. Solutions of desired concentration were prepared by diluting the stock solution.

2.3. Sorption batch experiments

Batch experiments were carried out to determine the optimum dosage and conditions for effective COD reduction. Equilibrium and kinetic studies were also carried out to determine the extent and mechanism of adsorption. For this, LAS-AC was added at a dosage of 10 mg to 800 mg into the conical flasks containing 20 ml of diluted spent wash solution and the flasks were placed in a thermostatic orbital shaker at 150 rpm to achieve equilibrium. After reaching equilibrium, the samples were taken out,filtered and analyzed for COD and pH. Based on the trial experiments, optimum conditions were obtained as follows: pH 5.5, dosage 50 mg, and time 60 min. After adjusting for pH, 50 mg of LAS-AC in 20 mL of spent wash solution having concentrations in the range of 25 to 180 mg/L were taken in the closed containers for isotherm studies. All the experiments were carried out at 25°C.

3. Results and discussion

3.1. Estimation of surface adsorption rate on LAS-AC

The rate at which the surface area of the sorbent is utilized for contaminant removal depends on the availability of potentially active sites [28]. It is essential to determine the surface interaction potential for the range of organic materials present in the spent wash and the predominant mass exchange mechanism within the given reaction time. Like any other sorbent, LAS-AC also showed significant dependence on solution pH while estimating the adsorption rate as well as adsorption capacity.

Since spent wash is highly acidic in nature with a pH 3.5 to 5 consisting of high concentrations of organic carbon, cationic nutrients, heavy metals, fermentation by-products and many organic acids, presence of active functional groups may facilitate polar interactions during initial phase of adsorption [48]. According to Malarvizhi and N. Sulochana (2008), the FTIR spectrum of LAS-AC constitutes of different bands of aliphatic C–H, C=O and N–H groups with frequency values of 2924, 1704 and 1614 cm^{-1} respectively. There were also evidences for the presence of phenolic OH and $–SO_3H$ groups at around 1383 and 620 cm^{-1} respectively [46]. As per Sartape et al. (2013), FTIR spectrum revealed the presence of –OH, C–H, C=O, C=C and C–C functional groups between 1041–3406 cm^{-1} range. The adsorption capacity was observed to be maximal (46.6 mg/g) at a pH of 5.5, owing to the high uptake rate of pollutants by the anionic functional groups in LAS-AC [12].

Based on the results from the batch kinetic studies, a number of commonly used kinetic models were developed to evaluate the adsorption rate.

The first order (FO) kinetic equation can be written as;

$$\log\left(q_e\right) = \log q_0 - k_1 t \tag{1}$$

where k_1 is the kinetic rate constant (min^{-1}) and q_e and q_0 (mg/g) are the amounts adsorbed at equilibrium and at time t (min) respectively.

Similarly, the second order (SO) kinetic equation can be written as;

$$\frac{1}{q_e} = \frac{1}{q_0} + 2k_2 t \tag{2}$$

where k_2 is the kinetic rate constant (min^{-1}).

First order (FO) and second order (SO) models were believed to predict specific rate of agro-based activated carbons with the assumption that reactions are reversible and uniform surface area and specific adsorption capacity are not the limiting factors. However, as evident from literature, pseudo first order and pseudo second order models are quite successful for LAS-AC sorption studies [44–47].

Linear form of Lagergren's pseudo first order (PFO) model is given by;

$$\log\left(q_e - q\right) = \log q_e + \frac{k_3 t}{2.303} \tag{3}$$

where k_3 is the PFO rate constant of adsorption (min^{-1}) and q is the amount adsorbed at time t (min).

Similarly, linear form of pseudo-second order (PSO) model can be written as;

$$\frac{t}{q} = \left(\frac{1}{q_e}\right)t + \frac{1}{k_4 q_e^2} \tag{4}$$

where k_4 is the PSO rate constant of adsorption (g/mg·min).

It is observed that FO and PFO models resulted in negative slopes giving minimum values of sorption rate constants whereas SO and PSO models predicted similar rate constants but with positive slope (Figs. 1a–d and Table 1). As literature review revealed, PSO is considered as the best fit model representing the evidence of chemi-sorption [39,49].

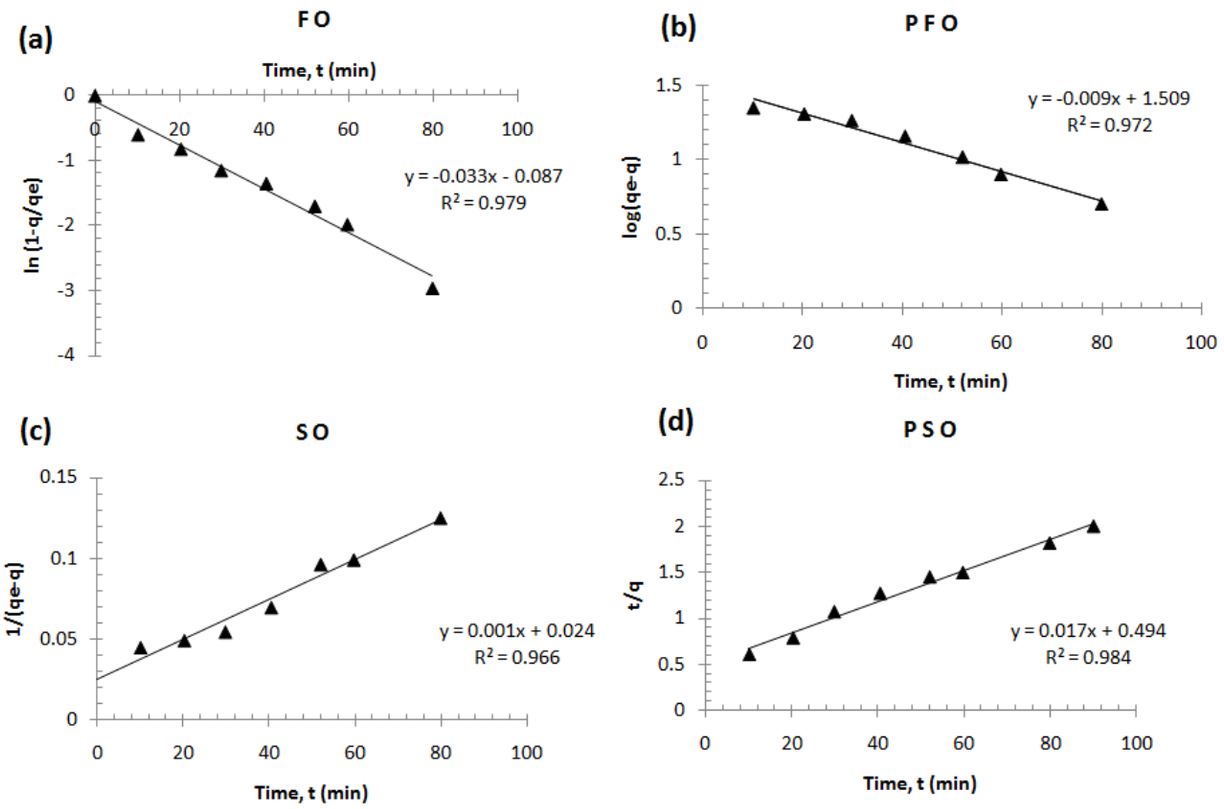

Fig. 1. Adsorption plots for different kinetic models ((a) FO - First order, (b) PFO - Pseudo first order, (c) SO - Second order, (d) PSO - Pseudo second order).

Table 1
Details of sorption kinetic models and derived parameters

Kinetic model	Slope	Intercept	R^2	Sorption capacity term (mg/g)	Sorption rate term (min^{-1})
FO	–0.033	–0.087	0.979	46.400	0.033
SO	0.001	0.024	0.966	41.667	0.001
PFO	–0.009	1.509	0.972	32.285	0.021
PSO	0.017	0.494	0.984	58.824	0.001
IPD	3.873	8.732	0.986	0.766*	3.873
Elovich	15.300	–22.860	0.973	65.359	3.434
TSSI	–0.012	–2.308	0.992	90.954	0.109
TSPI	–0.013	–3.361	0.991	96.530	0.125

*Initial adsorption factor

Considering the mass transfer rate based on reaction kinetics, both FO and PFO resulted in higher rate (0.033 and 0.021 min^{-1}) compared to SO and PSO (0.001 min^{-1}) (Figs. 1a–b). It is observed that FO and PFO models resulted in negative slopes (–0.033 and –0.009) and lesser values for sorption capacity terms (46.4 and 32.3), whereas SO and PSO models predicted similar rate constants but with gentler positive slopes (0.001 and 0.017) and higher sorption capacity terms (41.7 and 58.8 respectively) (Figs. 1c–d and Table 1). As the initial phase of adsorption is essentially limited by film and pore diffusion processes, understanding the nature of bulk mass transfer is important to determine the mass transfer limitation in reaching equilibrium.

3.2. Mass transfer limitations

Based on the major consecutive mass transport steps associated with the adsorption, sorption into interior sites very rapid; hence, film and pore transports are considered as the major steps controlling the rate of adsorption. In order to understand the effect of intra-particle diffusion over pH-mediated chemical reactions and to identify rate-limiting step, intra-particle diffusion (IPD) model and Elovich model were compared (Figs. 2a–b).

IPD model is given by:

$$q = k_d t^{0.5} + \theta \quad (5)$$

where k_d is the rate constant of the intra-particle transport and θ is the constant denoting the extent of initial adsorption. As the IPD curve does not pass through the origin, diffusion can be considered as the rate-limiting step [35]. It was observed that adsorption rates were highly over-predicted by these models owing to the large slope values. The intercept in IPD is generally accepted as a measure of the boundary layer thickness, which indicates the occurrence of large initial adsorption [50]. As evident from Figs. 2a and b,

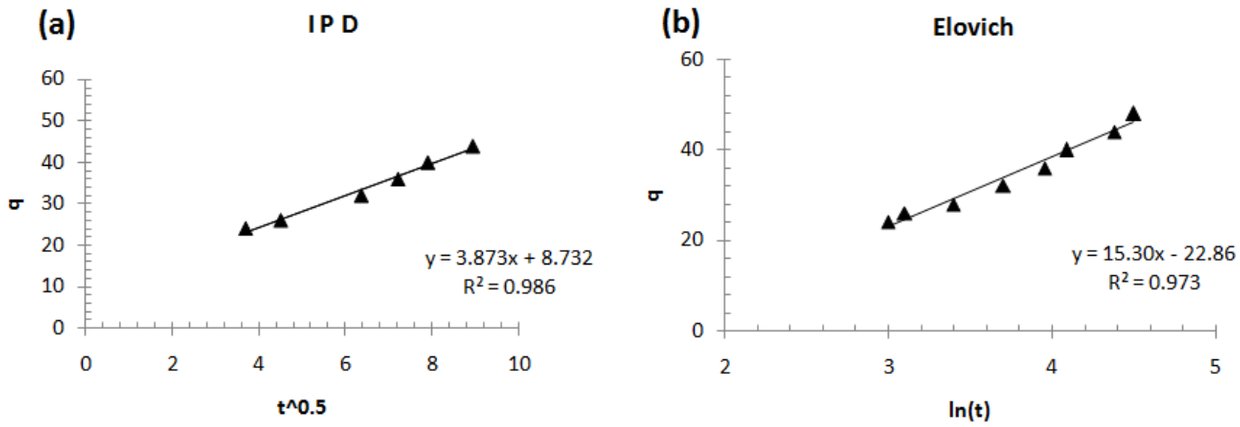

Fig. 2. Comparison of adsorption kinetics by (a) Intra-particle diffusion (IPD) model and (b) Elovich model.

the relation is not necessarily linear and there exists zones of varying mass transfer rate. Based on the intermediate range of initial adsorption factor (0.766), it can be observed that there may be slight intermediate rate of adsorption during the initial phase.

In a similar way, Elovich's model can be expressed as;

$$q = \left(\frac{1}{b_e}\right)\ln(t) + \left(\frac{1}{b_e}\right)\ln(a_e b_e) \tag{6}$$

where a_e is the initial adsorption rate (mg/g·min), and the parameter b_e is related to the extent of surface coverage and activation energy for chemi-sorption (g/mg). The sorption capacity term predicted by these kinetic models was comparable in general, while the highest values observed for Elovich and PSO models (Table 1).

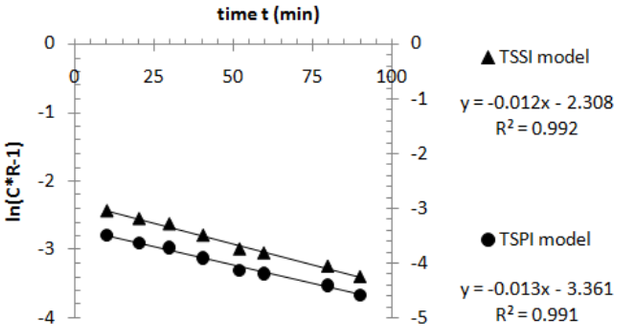

Fig. 3. Comparison of sorption kinetics using Two-Site series interface (TSSI) and Two-Site parallel interface (TSPI) models.

3.3. Multi-site kinetic mass transfer models

Apart from the variation in the initial rate of adsorption, mechanism and pathway of adsorption can also vary during the later stage. It is observed from Figs. 2a and b that Elovich model also could adequately represent the chemi-sorption as with PSO model. However, it is observed from these figures, that there is some transition in the behaviour during the kinetic experiments which is not a single-step process and could not be simulated by any of these kinetic models. In order to identify the impact of the initial diffusion and subsequent chemi-sorption, two different multi-site sorption models were compared in this study based on the assumption that only a fraction of the surface sites will be available for instantaneous sorption while the remaining fraction is time-dependent [51]. Based on the orientation and attachment of the sorbate on the sorbent surface, two-site series interaction (TSSI model) and two-site parallel interaction (TSPI model) were considered [49,51].

The linear form of TSSI and TSPI can be expressed as

$$\ln\left(C^* R - 1\right) = -\left(K_r / \beta\right)t + \ln\left(1/\beta - 1\right) \tag{7}$$

$$\ln\left(C^* - 1/R\right) = -\left(\alpha/\beta\right)t - \ln(1-\beta) \tag{8}$$

where $C^* = C_e/C_0$; retardation factor, $R = 1 + MK/V$; M is the mass of sorbent (g); K_r is the sorption rate constant for TSSI model (h^{-1}); V is the volume of the solution (mL); α is the sorption rate constant (h^{-1}) for TSPI model and β is a model parameter corresponding to equilibrium fraction [49].

It was noted that both TSSI and TSPI models resulted in high mass transfer rate (0.109 and 0.125 min^{-1} respectively) as well as in high sorption capacity values (90.9 and 96.5 respectively) within the experimental conditions. It was observed that these models could give highest fit (R^2 value > 0.99, based on linear regression analysis) and resulted in largest sorptive capacity terms (Fig. 3 and Table 1). This postulates the need for studying the dynamic and reversible nature of sorption resulting in change in the mass transfer mechanism and thereby estimating the efficient mass transfer rate.

3.4. Suitability of non-linear multi-parameter isotherms

A comparison has been made here with different linear forms of the popular isotherms from literature. The general nature of all isotherms follows type-II curve indicating the presence of narrow micro-pores of AC- LAS. This is in confirmation with the observation by similar studies [48,52].

The Langmuir isotherm assumes that there is a uniform and constant binding of the sorbate in the adsorbent surface.

The linear form of Langmuir isotherm can be expressed in two forms as below:

$$\frac{C_e}{q_e} = \frac{1}{q_m}C_e + \frac{1}{kq_m} \quad \text{(Form-I)} \tag{9}$$

$$\frac{1}{q_e} = \left(\frac{1}{kq_m}\right)\frac{1}{C_e} + \frac{1}{q_m} \quad \text{(Form-II)} \tag{10}$$

where q_e is the equilibrium amount of solute adsorbed, C_e is the equilibrium concentration of contaminants in spent wash expressed as COD (mg/L) and q_m and b are constants which represent the maximum solid phase loading and the energy constant related to the heat of adsorption, respectively.

The BET isotherm can be expressed as;

$$q_e = \frac{KC_eq_o}{(C_s - C_e)\left[1 + (K-1)\left(C_e/C_s\right)\right]} \tag{11}$$

where C_s is the saturation concentration and K is the adsorption energy constant.

By comparing the two linear forms of Langmuir isotherms (From-I and Form-II), relation between $1/q_e$ and $1/C_e$ yielded high sorption capacity (250 mg/g) as well as high coefficient of regression (R^2 = 0.994)than the plot between C_e/q_e and C_e. There is notable difference in the fitting parameters as well as predicted adsorption capacity between the two linear forms of Langmuir isotherm (Figs. 4a, 4b). However, Form-1 was invariable found to match with the experimental results, which is also in agreement with literature [53].

The three-parameter adsorption isotherm suggested by Redlich and Peterson (known as R-P isotherm) is well acclaimed for its rational fit for a wide range of equilibrium sorption capacities and concentrations [35,46,53]. In order to understand the characteristics of linear forms of this isotherm model, both logarithmic and exponential forms were analyzed for goodness of fit. The linear forms of R-P isotherm can be expressed as;

$$\ln\left(bq_m\frac{C_e}{q_e} - 1\right) = n\ln(C_e) + \ln(b) \quad \text{(Form-I)} \tag{12}$$

$$\frac{C_e}{q_e} = \left(\frac{1}{q_m}\right)C_e^n + \frac{1}{bq_m} \quad \text{(Form-II)} \tag{13}$$

It is observed that logarithmic form of R-P isotherm (Form-I) resulted in better fit than the powered form (Form-II) (Figs. 4c, 4d). The coefficients involved in these forms were obtained by trial and error method. The value of q_m by R-P Form-I (318.6 mg/g) is in general agreement with maximum adsorption capacity predicted by Langmuir Form-I (Table 2). It was also observed that by fitting R-P Form-II, the power term n was closely matching with the power term of Freundlich isotherm (Table 2). The value of power term (n) indicates the high rate of chemi-sorption experienced at equilibrium conditions [50].

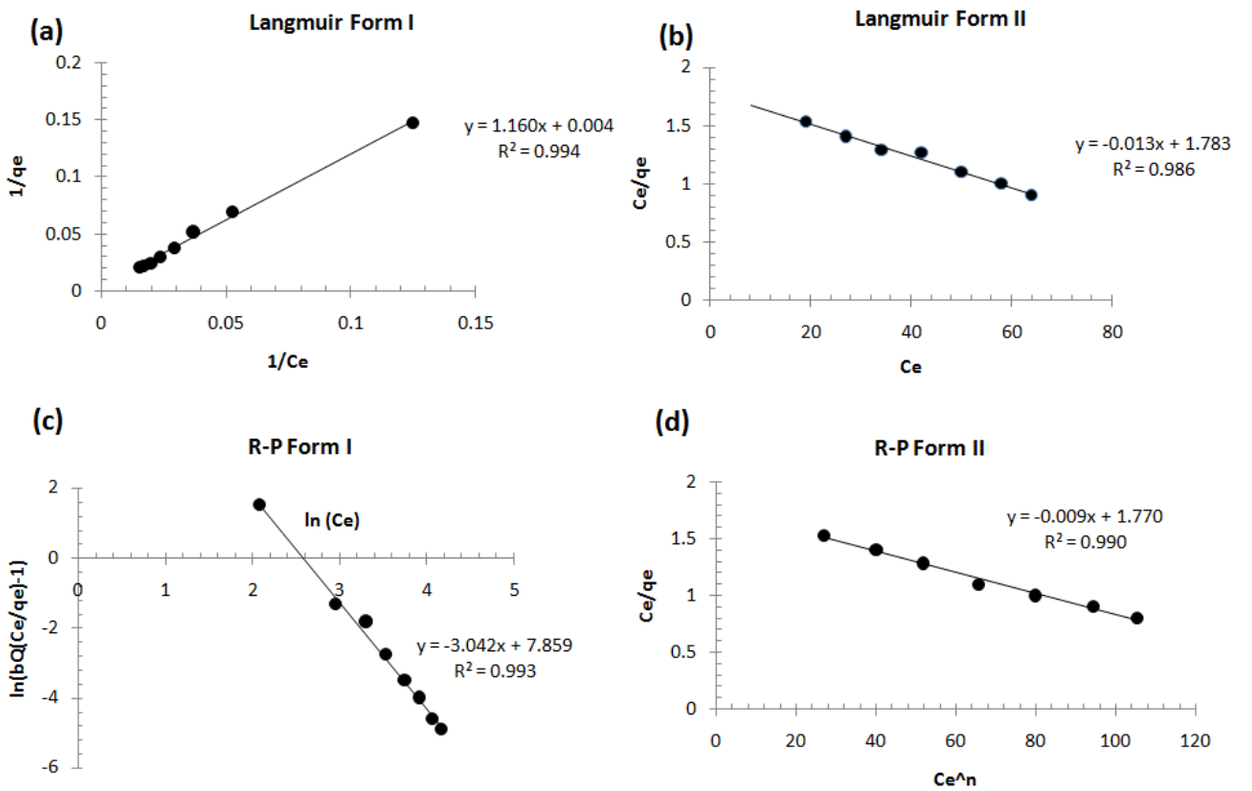

Fig. 4. Comparison between different linear forms of Langmuir ((a) Form-I, (b) Form-II) and Redlich-Peterson (R-P) ((c) Form-I, (d) Form-II) isotherms.

Table 2
Comparison of various isotherms and derived parameters

Isotherm	Slope	Intercept	R^2	χ^2	Sorption capacity term (mg/g)	Power term
Linear	0.765	–0.249	0.988	0.257		
Freundlich	0.953	0.039	0.994	2.401	0.914*	1.007
Langmuir Form I	1.160	0.004	0.994	0.673	250.000	–
Langmuir Form II	–0.013	1.783	0.986	14.476	156.923	–
R-P Form I	–3.042	7.859	0.993	0.214	318.664	1.042
R-P Form II	–0.009	1.770	0.990	0.172	211.111	1.120
BET	0.001	0.057	0.727	NC	172.414	1.018*

*Corresponds to Freundlich constant.

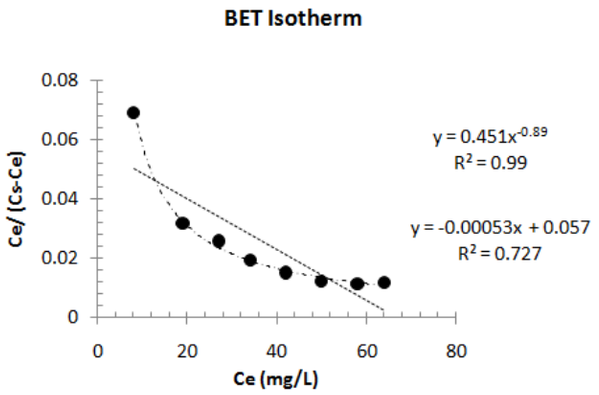

Fig. 5. Adsorption plot for identifying best fit form of BET isotherm.

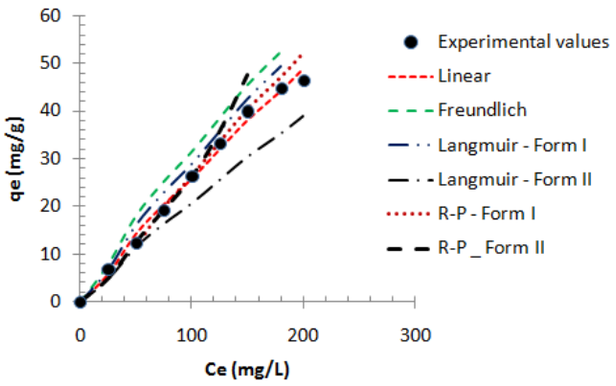

Fig. 6. Comparison of fitting of different isotherm models with experimental data.

Although R-P Form-I and Langmuir Form-I are unique in their asymptotic nature of isotherm for the selected range of COD concentrations, BET isotherm was exceptionally deviated with the selected data range (Table 2). However, it was observed that a powered form of the trend-line for the data resulted in very good fit (R^2 = 0.990) (Fig. 5). The value of the power-term is found to be 0.89. The reciprocal of the power-term in the fitting equation is observed to be well matching with the power term (n) in Freundlich model (Table 2). This further substantiate the argument that later phase of adsorption may be controlled by availability of active surface sites.

Within the selected ranges for spent wash concentration and LAS-AC dosage, it is clear that the nature of predominant adsorption mechanism at initial phase and later phase cannot be the same. The relatively higher values of equilibrium concentrations indicate delayed affinity of sorbent unto its surface owing to the limited surface potential for expanding the process at higher rate. It was observed that non-linear isotherms were unanimously predicting the initial range of parameters; however, the later phase of adsorption was better predicted by logarithmic forms of multi-parametric isotherms (Figs. 6 and 7).

A comparison of adsorption properties of wood apple for various sorbates was made in terms of isotherm and kinetic model parameters reported in literature (Table 3). The most common sorbates reported for wood apple include dyeing

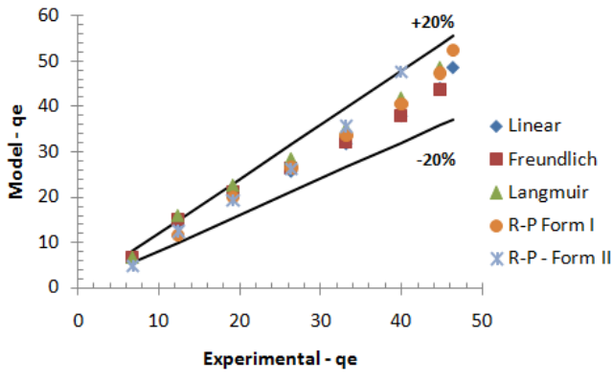

Fig. 7. Comparison of maximum error deviation between experimental and modeled values of q_e.

pigments and heavy metals. Within the optimum pH in the medium acidic range, optimum dosage was obtained as 500 mg. The maximum adsorption capacity terms from Langmuir and R-P isotherms were identified based on the linear regression fit as expressed by coefficient of determination (R^2). Apart from the general fit with the PSO model, TSSI/TSPI models were showing highest coefficient of determination, thereby explaining the mechanisms of multi-phase dynamic nature of adsorption.

Table 3
Comparison of adsorption properties of wood apple for various sorbates and their model parameters as reported in the literature

Adsorbate	Form of LAS	Mode of activation	Optimum conditions		Isotherm model parameters				Kinetic model parameters				Reference
			Dosage (mg)	pH	Best fit	Capacity term (mg/g)	Coefficient term (1/mg)	R^2	Best fit	Rate term	Capacity term (mg/g)	R^2	
Methylene blue	AC	H_2SO_4 at 160°C for 6 h	100	7.0	Langmuir	36.9	0.907	0.954	PSO	4–176 mg/mg/min	5–22	0.99	[46]
					R-P	31.5	0.839	0.956					
Methylene blue dye	As such	No chemical	100	6.9	Langmuir	95.2	0.059	0.997	PSO	5–8 mg/mg/min	97–128	0.999	[38]
Crystal violet dye	As such	No chemical	100	6.9	Langmuir	129.87	0.093	0.992	PSO	0.7–0.8 mg/mg/min	125–172	0.997	[38]
Malachite green dye	As such	No chemical	400	7.5	Langmuir	34.56	0.033	0.974	PFO	0.58×10^{-3} min^{-1}	12.35	0.92	[12]
Cadmium (II)	AC	H_2SO_4 for 1 h	400	6.5	Langmuir	28.33	0.0967	0.986	PFO	0.65×10^{-3} min^{-1}	12.35	0.98	[12]
Chromium (VI)	AC	H_2SO_4 at 300°C for 1 h	500	2.0	Langmuir	13.74	0.999	0.998	PFO	1.04×10^{-3} min^{-1}	9.77	0.967	[12]
Chromium (VI)	AC	H_2SO_4 at 600°C for 2 h	50	1.8	Langmuir	151.51	0.152	0.988	PSO	1.77–2.88 mg/mg/min	8–27	0.99	[45]
Fluoride	AC	Thermal at 600°C for 1 h	1500	7.0	Langmuir			0.831					[43]
Iron	AC	Thermal at 600°C for 1 h	2000	5.0	Freundlich			0.895					[44]
Spent wash	AC	H_2SO_4 at 200°C for 2 h	50	5.5	Langmuir	318.6	1.042	0.993	PSO	58.8 mg/mg/min	0.001	0.984	Present study
					R-P	250.0		0.994	TSSI/TSPI	90.5 mg/mg/min	0.1	0.99	

3.5. Use of chi-square test for comparison

Generally, most of the model fits are tested by coefficient of correlation and coefficient of determination [53]. Even though Langmuir and R-P isotherms could predict the trend of adsorption, there is notable difference in results while using different linear forms of these models. These linear equations had different axial settings individually so as to alter the result of linear regression fit. However, this difficulty can be overcome by using Chi-square (χ^2) test which makes comparison of all isotherms on the same abscissa and ordinate [53]. It was observed that Langmuir and R-P isotherms resulted in low values of χ^2 (less than 1), indicating a non-dimensional fit for the isotherm data within the range of experimental conditions (Table 2). Hence it is understood that use of non-linear χ^2-test can be a better method of checking the goodness of fit for adsorption isotherms.

4. Conclusions

Producing activated carbon from inexpensive raw material has gained massive attention. The main objective of this study was to evaluate the efficiency of activated carbon derived from wood apple in decontaminating aged distillery spent wash. Present study postulates the need for studying the dynamic and reversible nature of sorption resulting in change in the mass transfer mechanism and thereby estimating the efficient mass transfer rate. The key observations from the present study are as follows:

- Activated carbon with improved textural characteristics was obtained from wood apple shell.
- The batch experiments revealed that the adsorption capacity was observed to be maximal (46.6 mg/g) at a pH of 5.5, owing to the high initial uptake rate of polar-compounds from spent wash.
- Detailed analysis of experimental values of spent wash concentration and LAS-AC dosage revealed the nature of predominant adsorption mechanism at initial phase and later phase. The relative higher values of equilibrium concentrations indicate the delayed affinity of sorbent unto its surface owing to the limited surface potential for expanding the process at higher rate.
- It was observed that non-linear isotherms were unanimously predicting the initial range of parameters; however, the later phase of adsorption was better predicted by logarithmic forms of multi-parametric isotherms.
- By comparing different linear forms of isotherms, the variation in estimated sorption capacity could overcome by using Chi-square (χ^2) test which makes comparison of all isotherms on the same abscissa and ordinate.
- The study revealed that LAS-AC is a promising adsorbent for COD removal from distillery spent wash, thereby indicating the value addition of disposed shells for its reuse.

Acknowledgement

The authors deeply acknowledge the support and help rendered by the staff and management of Bannari Amman Institute of Technology, Sathyamangalam, Erode, India. The insightful and encouraging comments given by the anonymous reviewer is also acknowledged.

References

[1] M. Ludwig, E. Gould, Contaminant input, fate and biological effects, Woods Hole (MA): US Department of Commerce. NOAA/NMFS/Northeast Fisheries Science Center, NOAA Technical Memorandum NMFS-F/NEC., 7 (1988) 305–322.
[2] M.S. Islam, M. Tanaka, Impacts of pollution on coastal and marine ecosystems including coastal and marine fisheries and approach for management: a review and synthesis, Marine Poll. Bullet., 4 (2004) 624–649.
[3] Y.S. Wagh, N. Asao, Selective transfer semi-hydrogenation of alkynes with nanoporous gold catalysts, J. Org. Chem., 1 (2015) 847–851.
[4] Y. Zhou, S. Xia, J. Zhang, Z. Zhang, S.W. Hermanowicz, Adsorption characterizations of biosorbent extracted from waste activated sludge for Pb (II) and Zn (II), Des. Water Treat., 57(20) (2016) 9343–9353.
[5] N. Tewari, V.K. Verma, J.P. Rai, Comparative evaluation of natural adsorbent for pollutants removal from distillery spent wash, J. Sci. Ind. Res., 65 (2006) 935–938.
[6] N.S. Kumar, V. Thankamani, Characterization of molasses spentwash collected from United Spirits Ltd., Aleppey, India: a preliminary report, Int. J. Biotech. Biochem., 12(2) (2016) 103–110.
[7] G.S. Kumar, S.K. Gupta, G. Singh, Biodegradation of distillery spent wash in anaerobic hybrid reactor, Water Res., 2 (2007) 721–730.
[8] D. Pant, A. Adholeya, Biological approaches for treatment of distillery wastewater: a review, Biores. Tech., 9 (2007) 2321–2334.
[9] S.G. Pawar, G.R. Pathade, V.B. Rale, Pullulan production from cane molasses by *Aureobasidium mausonii* strain NCIM 1226, BioTech. Ind. J., 6(4) (2012) 111–114.
[10] Y. Satyawali, M. Balakrishnan, Removal of color from biomethanated distillery spent wash by treatment with activated carbons, Biores. Tech., 10 (2007) 2629–2635.
[11] R.K. Prasad, Color removal from distillery spent wash through coagulation using *Moringaoleifera* seeds: use of optimum response surface methodology, J. Hazard. Mater., 165(1) (2009) 804–811.
[12] A.S. Sartape, A.M. Mandhare, P.P. Salvi, D.K. Pawar, S.S. Kolekar, Kinetic and equilibrium studies of the adsorption of Cd (II) from aqueous solutions by wood apple shell activated carbon, Desal. Water Treat., 51(22–24) (2013) 4638–4650.
[13] S. Yadav, R. Chandra, Biodegradation of organic compounds of molasses melanoidin (MM) from biomethanated distillery spent wash (BMDS) during the decolourisation by a potential bacterial consortium, Biodeg., 7 (2012) 609–620.
[14] B.M. Krishna, U.N. Murthy, B.M. Kumar K.S. Lokesh, Study of the electrochemical process for distillery waste water treatment, J. Environ. Res. Develop., 5(1) (2010) 134–140.
[15] S. Mohana, C. Desai, D. Madamwar, Biodegradation and decolourization of anaerobically treated distillery spent wash by a novel bacterial consortium, Biores. Tech., 98(2) (2007) 333–339.
[16] S.T. Ramesh, R. Gandhimathi, J.H. Joesun, P.V. Nidheesh, Low cost biosorbent *'CyperusRotundus'* for removal of Cu (II) and Zn (II) from aqueous solution with acid and alkali treatments: kinetic and equilibrium studies, Adv. Porous Mater., 1 (2016) 46–53.
[17] D. Pant D, A. Adholeya, Concentration of fungal ligninolytic enzymes by ultrafiltration and their use in distillery effluent decolorization, World J. Microbio. Biotech., 10 (2009) 1793–1800.
[18] I.S. Chang, K.H. Choo, C.H. Lee, U.H. Pek, U.C. Koh, S.W. Kim, J.H. Koh, Application of ceramic membrane as a pretreatment in anaerobic digestion of alcohol-distillery wastes, J. Membr. Sci., 4 (1994) 131–139.

[19] A.D. Dhale, V.V. Mahajani, Treatment of distillery waste after bio-gas generation: wet oxidation, Indian J. Chem. Tech., 7 (2000) 11–18.
[20] T. Kumaresan, K.M. Begum, P. Sivashanmugam, N. Anantharamanand, S. Sundaram, Experimental studies on treatment of distillery effluent by liquid membrane extraction, Chem. Eng. J., 9 (2003) 199–204.
[21] S.K. Nataraj, K.M. Hosamani, T.M. Aminabhavi, Distillery wastewater treatment by the membrane-based nanofiltration and reverse osmosis processes, Water Res., 7 (2006) 2349–2356.
[22] A. Mandal, K. Ojha, D.N. Ghosh, Removal of colour from distillery wastewater by different processes, Ind. Chemical Eng., 45(4) (2003) 264–267.
[23] F.J. Beltran, A. Aguinaco, J.F. García-Arayaand A. Oropesa, Ozone and photocatalytic processes to remove the antibiotic sulfamethoxazole from water, Water Res., 8 (2008) 3799–3808.
[24] A.A. Kulkarni, Solar assisted photocatalytic oxidation of distillery waste, Ind. Chem. Eng., 40 (1998) 169–172.
[25] P. Turan Beyli, M. Dogan, M. Alkan, A. Turkyılmaz, Y. Turhan, O. Demirbaş, H. Namli, Characterization, adsorption, and electrokinetic properties of modified sepiolite, Desal. Water Treat., 57(41) (2016) 19248–19261.
[26] D. Krishnaiah, S.M Anisuzzaman, A. Bono, R. Sarbatly, Adsorption of 2,4,6-trichlorophenol (TCP) onto activated carbon, J. King Saud Univ. Sci., 7 (2013) 251–255.
[27] P. Ehrburger, A. Addoun, F. Addoun, J.B. Donnet, Carbonization of coals in the presence of alkaline hydroxides and carbonates: Formation of activated carbons, Fuel, 10 (1986) 1447–1449.
[28] A.M. Puziy, O.I. Poddubnaya, A. Martınez-Alonso, F. Suarez-Garcıa, J.M. Tascon, Synthetic carbons activated with phosphoric acid: I. Surface chemistry and ion binding properties, Carbon., 8 (2002) 1493–1505.
[29] C. Namasivayam, D. Kavitha, Removal of Congo Red from water by adsorption onto activated carbon prepared from coir pith, an agricultural solid waste, Dyes Pigments., 7 (2002) 47–58.
[30] J.F. Garcia-Araya, F.J. Beltran, P. Alvarez, F.J. Masa, Activated carbon adsorption of some phenolic compounds present in agro-industrial wastewater, Adsorption, 6 (2003) 107–115.
[31] Z. Hu, E.F Vansant, Carbon molecular sieves produced from walnut shell, Carbon, 1 (1995) 561–567.
[32] A.P. Carvalho, B. Cardoso, J. Pires, M. Brotas de Carvalho, Preparation of activated carbons from cork waste by chemical activation with KOH, Carbon, 41 (2003) 2873–2876.
[33] J. Guo, A.C. Lua, Preparation of activated carbons from oil-palm-stone chars by microwave-induced carbon dioxide activation, Carbon, 12 (2000) 1985–1993.
[34] A. Heidari, H. Younesi, A. Rashidi, A. Ghoreyshi, Adsorptive removal of CO_2 on highly microporous activated carbons prepared from Eucalyptus camaldulensis wood: effect of chemical activation, J. Taiwan Inst. Chem. Engg., 3 (2014) 579–588.
[35] D. Aravind, R. Krishna Prasad, Film pore diffusion modeling and contact time optimization for adsorption of distillery spentwash on fly ash, Desal. Water Treat., 57(52) (2016) 24925–24933.
[36] P. Amale, S. Kulkarni, K. Kulkarni, A review on research for industrial wastewater treatment with special Emphasis on distillery effluent, Int. J. Ethics. Eng. Manage Edu., 9 (2014) 1–4.
[37] S.J. Kulkarni, S.V. Patil, Y.P. Bhalerao, Fly ash adsorption studies for organic matter removal accompanying increase in dissolved oxygen, Int. J. Chem. Eng. App., 12 (2011) 434.
[38] S. Jain, R.V. Jayaram, Removal of basic dyes from aqueous solution by low-cost adsorbent: Wood apple shell (*Feronia acidissima*), Desalination, 1 (2010) 921–927.
[39] C. Suresh, D. Reddy, Y. Harinath, B.R. Naik, K. Seshaiah, A.V. Reddy, Development of wood apple shell (*Feronia acidissima*) powder biosorbent and its application for the removal of Cd (II) from aqueous solution, Sci. World J., 4 (2014) 1–8.
[40] Y. Zhou, Z. Zhang, J. Zhang, S. Xia, New insight into adsorption characteristics and mechanisms of the biosorbent from waste activated sludge for heavy metals, J. Environ. Sci., 45 (2016) 248–256.
[41] Y. Zhou, S. Xia, J. Zhang, B.T. Nguyen. Z. Zhang, Insight into the influences of pH value on Pb(II) removal by the biopolymer extracted from activated sludge, Chem. Eng. J., 308 (2017) 1098–1104.
[42] Y. Zhou, Z. Zhang, J. Zhang, S. Xia, Understanding key constituents and feature of the biopolymer in activated sludge responsible for binding heavy metals, Chem. Eng. J., 304 (2016) 527–532.
[43] G. Anusha, S.M. Kumar, Adsorption of iron from aqueous solution using *Limonia acidissima* fruit shell activated carbon as an adsorbent, Nat. Environ. Pol. Tech., 12 (2011) 637–638.
[44] G. Anusha, J. Murugadoss, Studies of the adsorption of fluoride and iron from aqueous solution using *Limonia acidissima* as adsorbent, J. Ind. Poll. Cont., 6 (2015) 47–50.
[45] K.M. Doke, E.M. Khan, Equilibrium, kinetic and diffusion mechanism of Cr (VI) adsorption onto activated carbon derived from wood apple shell, Arab. J. Chem., 8 (2012) S252–S260.
[46] R. Malarvizhi, N. Sulochana, Sorption isotherm and kinetic studies of methylene blue uptake onto activated carbon prepared from wood apple shell, J. Environ. Prot. Sci., 2 (2008) 40–46.
[47] S. Karthikeyan, P. Sivakumar, The effect of activating agents on the activated carbon prepared from *Feronia limonia* (L.) Swingle (Wood Apple) shell, J. Environ. Nanotechnol., 1(1) (2012) 5–12.
[48] F. Ansari, A. K. Awasthi, P.B. Srivastava, Physico-chemical characterization of distillery effluent and its dilution effect at different levels, Arch. App. Sci. Res., 4 (2012) 1705–1715.
[49] M. Vasudevan, P.S. Ajithkumar, R.P. Singh, N. Natarajan, Mass transfer kinetics using two-site interface model for removal of Cr(VI) from aqueous solution with cassava peel and rubber tree bark as adsorbents, Env. Eng. Res., 2 (2016) 152–163. DOI: 10.4491/eer.2015.152.
[50] F.C. Wu, R.L. Tseng, R.S. Juang, Initial behaviour of intra-particle diffusion model used in the description of adsorption kinetics, Chem. Eng. J., 11 (2009) 1–8.
[51] S.M. Lee, C. Laldawngliana, D. Tiwari, Iron oxide nano-particles-immobilized-sand material in the treatment of Cu(II), Cd(II) and Pb(II) contaminated waste waters, Chem. Eng. J., 7 (2012) 103–111.
[52] S.J. Gregg, K.S. Sing, Adsorption surface area and porosity, Academic Press, New York, 1982.
[53] Y.S. Ho, Selection of optimum sorption isotherm, Carbon, 12 (2004) 2115–2116.